Eighth Australasian Fluid Mechanics
Conference, University of Newcastle,
N.S.W., 28 November/2 December 1983.

THE EFFECTS OF FRICTION ON CURRENTS OVER SHALLOW CONTINENTAL SHELVES

E. WOLANSKI

AUSTRALIAN INSTITUTE OF MARINE SCIENCE

TOWNSVILLE, QLD. 4810 AUSTRALIA

SUMMARY Analytical models of barotropic wind-driven and tidal currents on the continental shelf of the northern and central regions of the Great Barrier Reef have been calibrated against field data to yield the value of the bulk bottom friction coefficient, C_d. The value of C_d depends not only on the tidal stress but also on the 'roughness' as defined by the 'density' of the coral reefs scattered on the continental shelf. As a result, the wind-driven continental shelf waves found in the central region degenerate into arrested topographic waves in the northern region.

1 INTRODUCTION

As part of the research program in physical oceanography by the Australian Institute of Marine Science, I have run, with various co-workers, long-term studies of water circulation over the continental shelf of the Great Barrier Reef (GBR). The study sites are in the GBR central region (16° to 20°S lat., Fig. 1) from 1980 to 1982, and the northern region (9° to 15°S lat., Fig. 2) in 1979 and in 1981 to 1982. The studies involve the deployment and maintenance for more than one year of a large number of self-recording current meters, water level recorders and weather stations, at sites shown in Figs. 1 and 2. Some pertinent results on the effects of friction are summarized below; more details can be found in the references.

The results from the central and northern regions will be described separately, because of the different water circulation patterns in both regions, due to different topographies. In the central region, coral reefs are concentrated in a wide (≈30-60 km) matrix at the shelf break. This matrix is quite porous, as there are wide (several km) and deep (≈50 m) passages between the reefs. There exists a wide (≈60 km) fairly deep (≈30-40 m) reef-free lagoon between the shore and the reef. In the northern region (see slides), coral reefs form the outer Great Barrier Reef along the shelf break, cut by passages (≈30-40 m deep) occupying 10-30% of the shelf break length. In addition, reefs and submerged sand banks are also scattered often very densely throughout the shelf width, mean water depth being ≈20-30 m.

2 THE CENTRAL REGION

In the trade wind season, the dominant wind direction changes from westward over the Coral Sea to northwestward over the shelf. The dominant wind component is highly coherent over distance of at least 1500 km, with negligible time lags from site to site so that the wind-field over the shelf can be treated as time-dependent but stationary. The wind is energetic at all periods from 6 to 200 days.

Baroclinic effects on the currents are most significant near the shelf break. The thermocline in the Coral Sea is located at 80-100 m depth. Typical time series of low-frequency (tidal-averaged) sea level and longshore currents are shown in Fig. 3. Large fluctuations of low-frequency longshore currents (up to 80 cm s^{-1}) and sea level (up to 35 cm) lasting typically one to two weeks are observed. (I have collected a 2.3 year long continuous time series of currents and wind to

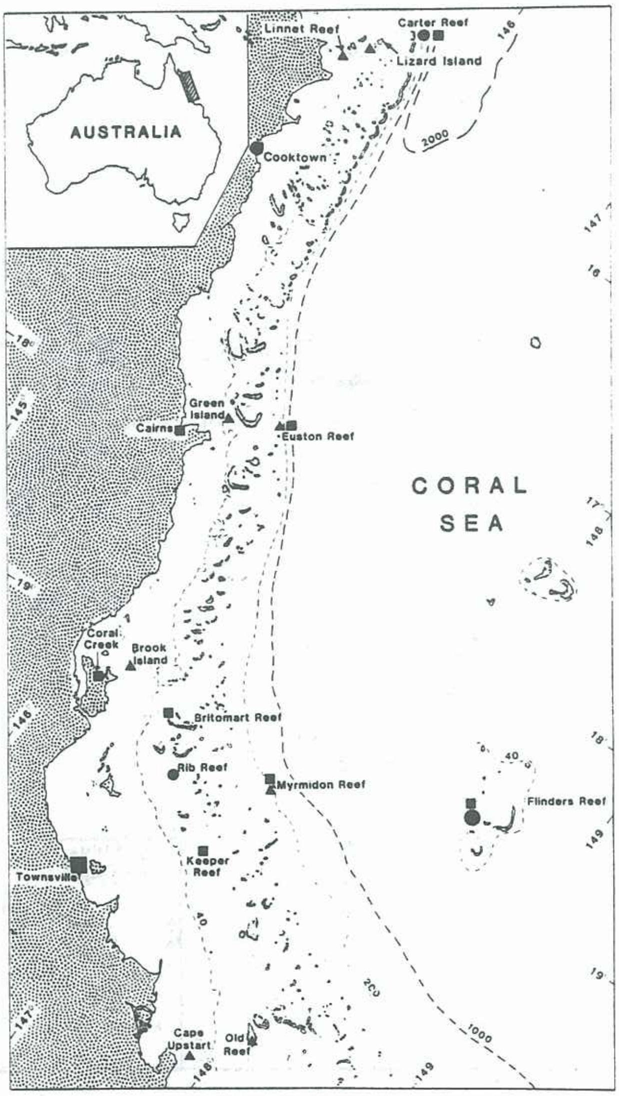

Fig. 1: Map of the central region of the GBR, showing location of tide gauges (■), weather stations (●) and current meters (▲).

investigate even longer periods of fluctuations.) Figs. 4 and 5 show, as example, the coherence between currents off Cape Upstart and Green Island and between sea level at Townsville and Carter Reef (about 1 year of data). The sea level and current fluctuations were propagating longshore northward at speeds ≈450 km day^{-1}, independent of the period.

A term balance analysis was carried out of the f-plane shallow water wave equations, to show that over the shelf, the equations of motion for wind-driven currents reduce to

$$-fv = -gh_x - F^x/H \quad (1)$$

$$v_t + fu = -gh_y + T^y/H - F^y/H \quad (2)$$

$$(Hu)_x + (Hv)_y = 0 \quad (3)$$

where t is the time, x and y the horizontal cartesian coordinates (x is cross-shelf pointing offshore, y longshore northward), u and v the velocity components, F^x and F^y the bottom friction components and T^y the wind stress. A subscript indicates a partial derivate, g the acceleration due to gravity, H the undisturbed water depth, h the sea level disturbance, f the Coriolis parameter. Taking

$$(F^x,\ F^y) = r\ (u,v) \quad (4)$$

where r is a friction parameter, and, for the forcing,

$$T^y = (0, y<0;\ T_o \exp(i\omega t),\ 0<y<A;\ 0,\ y>A) \quad (5)$$

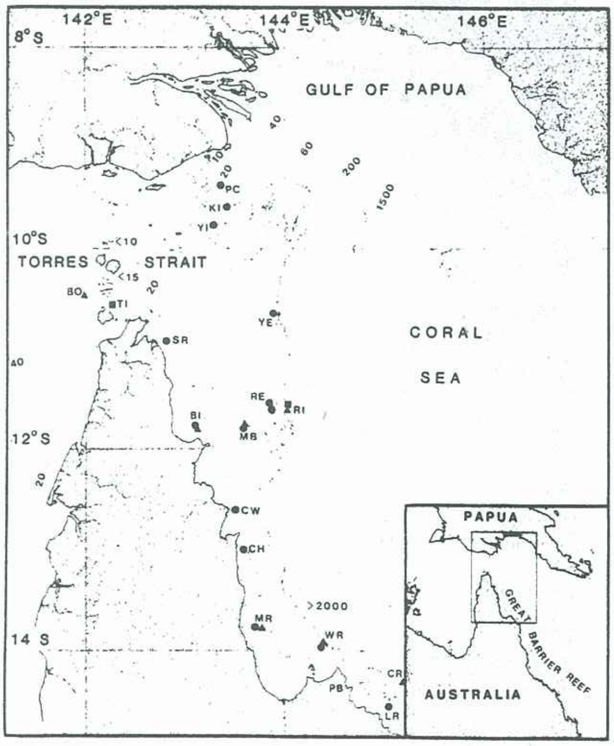

Fig. 2: Map of the northern region of the GBR. (●) current meters, (■) weather station, (▲) tide gauges.

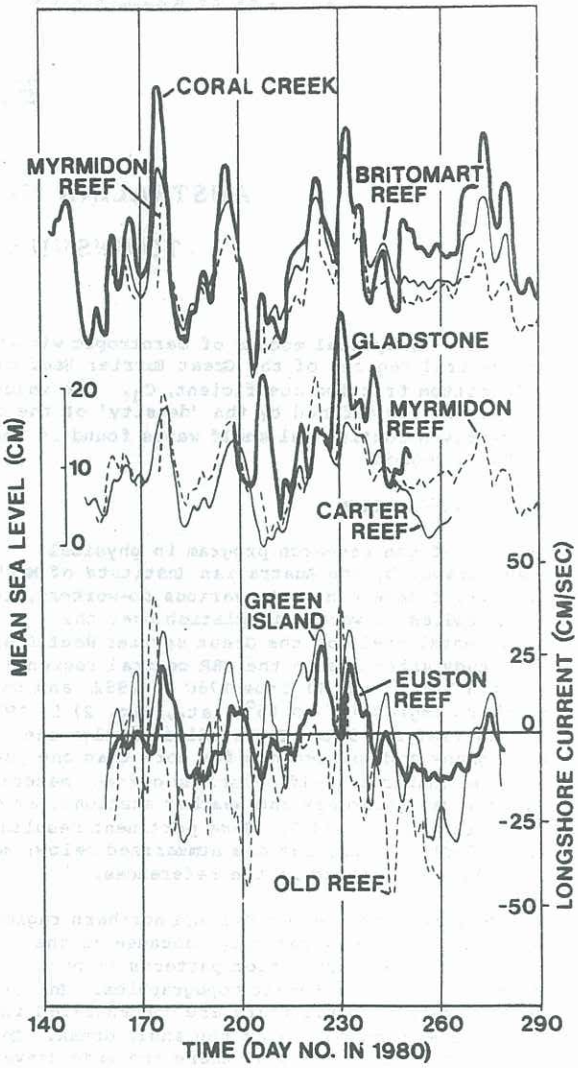

Fig. 3: Typical time series of low-frequency sea level and longshore currents.

where ω is the frequency, A the size of the wind-field, T_o a constant, $i = (-1)^{1/2}$. For a shelf of width L and constant depth $H_s << H_o$, where H_o is the ocean depth, assuming continuity of h and uH at x = L, and h → o as x → ∞, the solution is

$$u = -x\ v_y \quad (6)$$

$$h = (x - L)\ fv/g \quad (7)$$

$$v = B \exp(i\omega t)\ (1-\exp(-i\omega y/c)\ \exp(-by/c) \quad (8)$$

where $B = (T_o/H_s)/(i(\omega - ib))$, $b = r/H_s$, $c = -fL$. This simple model produces results that agree well with a number of observations (see slides). The observed overall decay of a shelf wave amplitude as it travels northward is best modelled for $r \approx 2 \times 10^{-4}$ m s^{-1}, or, assuming

$$(F^x,\ F^y) = C_d |\underset{\sim}{u}^*| (u,v) \quad (9)$$

where $\underset{\sim}{u}^*$ is the root-mean-square velocity (comprising both high and low frequency motions),

$$C_d \approx 0.002 \quad (10)$$

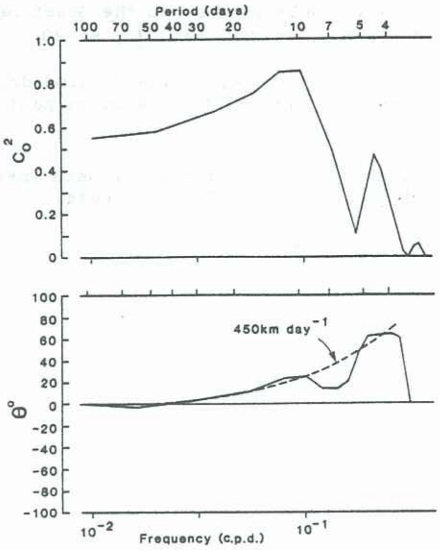

Fig. 4: Square coherence (C_o^2) and phase (θ) between low-frequency longshore currents off Cape Upstart and Green Island ($\simeq$ 1 year of data). 95% confidence level for $C_o^2 \simeq 0.4$, at 10 day period.

3 THE NORTHERN REGION

The value of C_d was determined separately from the low-frequency wind-driven and the tidal currents. As is shown in the slides, the semi-diurnal tides dominate the tidal signal. Along the shelf break, the longshore gradient of amplitude and phase of the tidal constituents is very small, and, except in reef passages, tidal currents are small. Near the coast, the longshore tidal currents are strong and strong longshore gradients of phase and amplitude are observed, clearly related to the increase in shelf width with latitude, mostly, between 12 and 10^oS. These properties can be modelled as follows.

Using a shelf-averaged bottom friction law, the equations of motion are (Battisti and Clarke, 1982)

$$u_t - fv = -gh_x - \lambda_o u \quad (11)$$

$$v_t + fu = -gh_y - \lambda_o v \quad (12)$$

$$h_t + (Hu)_x + (Hv)_y = 0 \quad (13)$$

where $\lambda_o = r/H$ is assumed constant. Taking

$$(u,v,h) = (u_{o(x,y)}, v_{o(x,y)}, h_{o(x,y)})\exp(i\omega t) \quad (14)$$

assuming that ℓ is a constant, where

$$i\ell = h_y/h \quad (15)$$

and that $h_{yy} << h_{xx}$, it is possible to find a solution in terms of zero order Bessel functions of x. To reproduce in the model the cross-shelf amplication of the M_2 tide, or the M_2 longshore coastal current (see slides), best fit techniques yield $\lambda_o \simeq 3 \times 10^{-4}\ s^{-1}$, or roughly,

$$C_d \simeq 0.01-0.03 \quad (16)$$

The second estimate of C_D is derived from an analysis of the term balance in the equations of motion for wind-driven currents. This time, contrary to the situation in the central region, the term v_t is negligible in the longshore momentum eq. (2). Travelling waves thus cannot exist, and indeed are not observed (see slides), and only quasi-steady arrested topographic waves are present (e.g. Csanady, 1978). 'Upstream' and 'downstream' boundary conditions are needed to solve the equations. The model based on eqs. (1) to (3), neglecting v_t, yields a favourable comparison between observed and computed currents (Fig. 6), for

$$C_d \simeq 0.05 \quad (17)$$

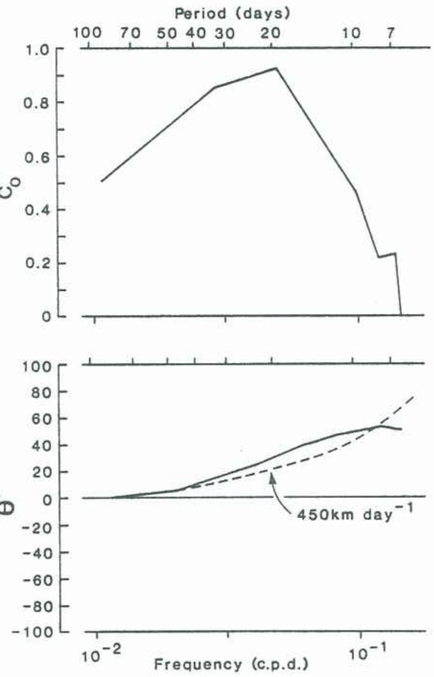

Fig. 5: Square coherence and phase between low-frequency sea level at Townsville and Carter Reef.

4 DISCUSSION

From eqs. (10), (16) and (17), it is clear that the value of C_d is one order of magnitude higher in the northern than in the central region. This difference results in a different response of the two regions to the wind forcing, and is due to the greater energy dissipation by the secondary circulation around islands and reefs in the densely reef-studded northern region than in the fairly reef-free central region.

5 ACKNOWLEDGEMENTS

Publication No. 139 from the Australian Institute of Marine Science.

6 REFERENCES

BATTISTI, D.S. and CLARKE, A.J. (1978) Estimation of nearshore tidal currents on non-smooth continental shelves. J. Geophys. Res. 87, 7873-7878.

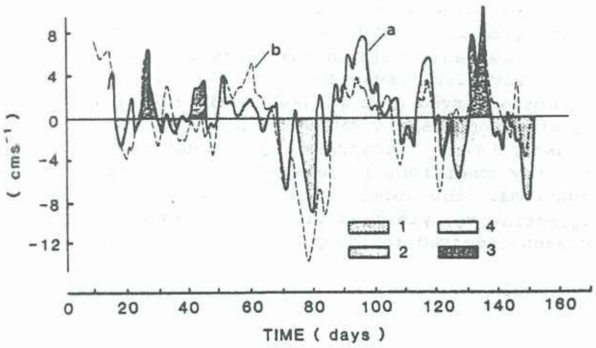

Fig. 6: Observed (a) and computed (b) longshore currents. The 4 shading codes will be explained in slides.

CSANADY, G.T. (1978) The arrested topographic wave. J. Phys. Ocean. 8, 47-62.

WOLANSKI, E. (1982) Low level trade winds over the western Coral Sea. J. Appl. Meteor. 21, 881-882.

WOLANSKI, E. and BENNETT, A.F. (1983) Continental shelf waves and their influence on the circulation around the Great Barrier Reef. Aust. J. Mar. Freshw. Res. 34, 23-48.

WOLANSKI, E. and PICKARD, G.L. (1983) Upwelling by internal tides and Kelvin waves in the Great Barrier Reef. Aust. J. Mar. Freshw. Res. 34, 65-80.

WOLANSKI, E. and THOMSON, R.E. (1983) Wind-driven circulation on the northern Great Barrier Reef continental shelf in summer.

WOLANSKI, E. (1983) Tides on the northern Great Barrier Reef continental shelf. In press.